frontiers in Earth Science

BRIEF RESEARCH REPORT
published: 19 March 2021
doi: 10.3389/feart.2021.645061

The Cantabrian Fault at Sea. Low Magnitude Seismicity and Its Significance Within a Stable Setting

Gabriela Fernández-Viejo, Sergio Llana-Fúnez, Jorge Acevedo and Carlos López-Fernández*

Department of Geology, University of Oviedo, Oviedo, Spain

The Cantabrian fault (CF) is a crustal-scale structure that cuts obliquely the western North Iberian Margin (NIM) for 160 km and continues onshore transecting the Cantabrian Mountains (CM) for another 150 km as the Ventaniella fault (VF). For most of its length inland, the fault system is aseismic, except for a 70 km long segment at its southern end. Within this segment, a gently north-dipping linear arrangement of earthquakes was interpreted as related to the intersection of a slightly oblique fault to VF with the basal thrust of the CM. In addition to earthquake nucleation along parts of its length, the CF–VF also stands out regionally as a major seismotectonic boundary, separating a seismically active area to the West from an essentially aseismic region to the East. Contrasting tectonothermal evolution in the crust on either side during the Mesozoic rifting may underlie the observed differences. On the other hand, the seismicity within the subsea segment is low magnitude, persistent, and understudied. The scarcity of the permanent seismic stations distribution in the area did not allow to establish more than a generalized consensus relating the offshore events to the submarine structure. A recent local seismic network monitored the area providing the highest accuracy information on the offshore events to date. Although the location of foci is partially challenged by the lack of recording stations from northern azimuths at sea, the observed pattern shows indeed a broad linear trend in the submarine domain in relation to the crustal-scale structure. Specifically, this study shows that the distribution of foci offshore display two preferential areas along the CF–VF within its southern crustal block. Considering the basement rock types and the deep architectural disposition of the margin crust, two possible explanations for the origin of the clusters are put forward in this contribution.

Keywords: Cantabrian fault, Bay of Biscay, Ventaniella fault, intraplate seismicity, North Iberian Margin

OPEN ACCESS

Edited by:
Sara Martinez-Loriente, Instituto de Ciencias del Mar, Consejo Superior de Investigaciones Científicas (CSIC), Spain

Reviewed by:
Sónia Silva, Portuguese Institute for Sea and Atmosphere (IPMA), Portugal
Steano Tavani, University of Naples Federico II, Italy

****Correspondence:***
Gabriela Fernández-Viejo
fernandezgabriela@uniovi.es

Specialty section:
This article was submitted to Structural Geology and Tectonics, a section of the journal Frontiers in Earth Science

Received: *22 December 2020*
Accepted: *01 March 2021*
Published: *19 March 2021*

Citation:
Fernández-Viejo G, Llana-Fúnez S, Acevedo J and López-Fernández C (2021) The Cantabrian Fault at Sea. Low Magnitude Seismicity and Its Significance Within a Stable Setting. Front. Earth Sci. 9:645061. doi: 10.3389/feart.2021.645061

INTRODUCTION. TECTONIC SETTING

The opening of the Atlantic Ocean initiated in the late Jurassic to early Cretaceous and had several aborted branches. The northern coast of the Iberian Peninsula constitutes the southern margin of one of these aborted rifts: the Bay of Biscay. The opening of the Bay of Biscay, progressing from West to East, produced the hyperextension of the northeastern part of the Iberian Peninsula leaving a strong thermal imprint in the crust (e.g., Tugend et al., 2014; Cadenas et al., 2018). The margin includes different rift systems which based on a tectono-stratigraphic analysis

(Cadenas et al., 2020), can be summarized into (1) an early diffuse widespread Triassic system, (2) a confined Late Jurassic to Barremian left-lateral transtensional one, and (3) a wide Aptian to Cenomanian hyperextended rift system. The inherited templates guided the subsequent events and the spatial distribution and overprint of the systems results in a complex 3D structure. However, west of the Ventaniella fault (VF)–Cantabrian fault (CF), in the area targeted in this study, the later systems were less important than to the East, and the variscan basement therefore, considerably less affected thermally and tectonically.

During the Cenozoic, the Bay of Biscay hosted the convergent plate boundary between the Iberian and the Eurasian plates (Srivastava et al., 1990). The deformation associated to this convergence stage was strongly localized in the southern margin of the rift, reversing some of the extensional movements or, in many cases, partially overprinting earlier structures (e.g., Boillot et al., 1979). The interplay of the Alpine compression with the three Mesozoic rifting systems amplified the inherited differences and segmentations providing the ample variations observed along the margin today. With compression, an accretionary wedge formed at the bottom of the slope (Álvarez-Marrón et al., 1997), representing one of the few margins in the world that preserves such a witness of early reactivation (Stern and Gerya, 2018). The wedge increases in extension and depth toward the east (Fernández-Viejo et al., 2012). The compression was halted when the plate boundary migrated to the south in the actual Azores-Gibraltar zone.This fact makes the North Iberian Margin (NIM) one of the best examples where polyphase-multistage rifting and posterior reactivation processes can be investigated, as the later tectonic events did not obliterate completely the earlier extensional structures (Roca et al., 2011; Tugend et al., 2014; Cadenas et al., 2020).

Prior to the Mesozoic extension, the basement in North Iberia was characterized by the Variscan orogenesis during the Carboniferous in this part of the ancient mountain belt (**Figure 1**). The structural grain of the Variscan orogen observed onshore is northerly to northwesterly oriented for most of the western half of the Peninsula turning northeasterly offshore (Pérez-Estaún et al., 1991). The latest major tectonic Variscan structure in northwestern Iberia dates from the early Permian (e.g., López-Sánchez and Llana-Fúnez, 2018). More than 50 ma later, in the Late Permian, the nascent rift cut obliquely across major variscan structures (Arche and López-Gómez, 1996) producing several northwesterly trending faults with minor basins and associated local volcanism (Martínez-García et al., 2004).

Crustal Structure

The thickness of the crust in the north-western corner of the Iberian Peninsula is fairly constant, with the Moho discontinuity located at about 32 km depth on land (Cordoba et al., 1988; Fernández Viejo et al., 2000). Within the continental platform west of VF–CF, crustal thickness reduces slightly to 27–9 km (Ayarza et al., 1998). The crust-mantle boundary remains nearly

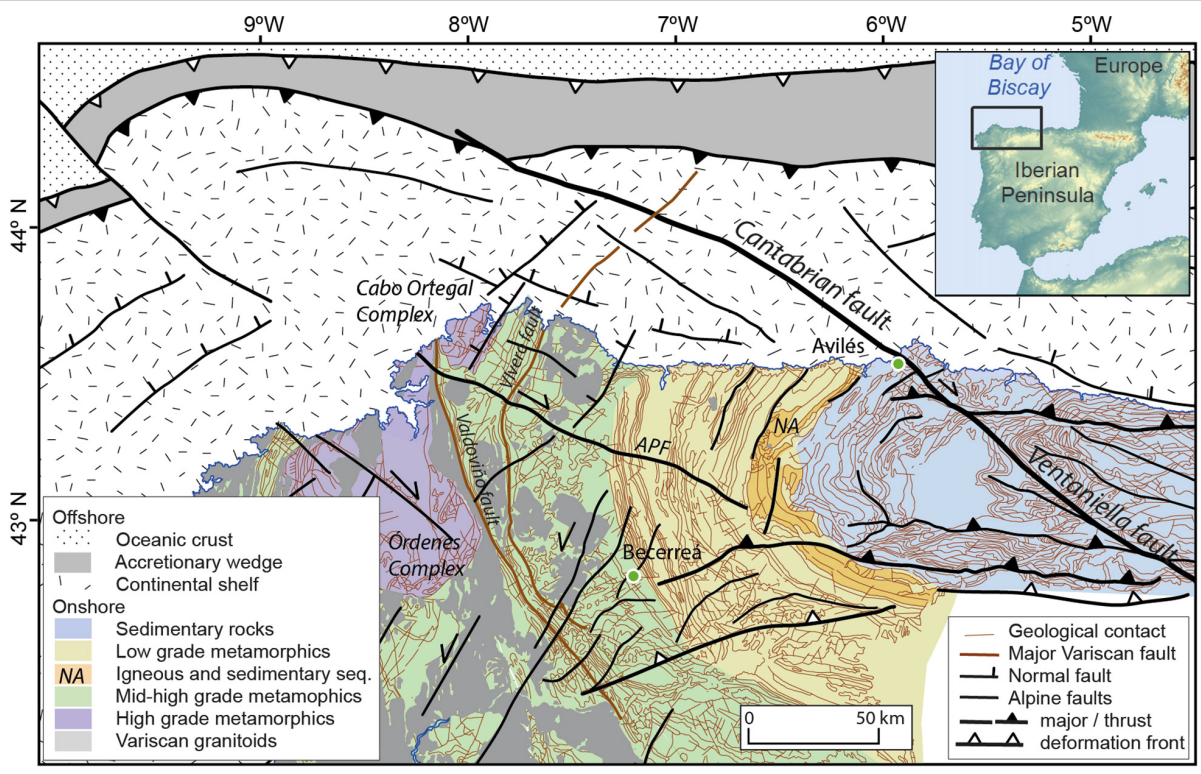

FIGURE 1 | Geological map of the Northwest Iberian Peninsula and margin. The trace of the Cantabrian fault according to Fernández-Viejo et al. (2014). APF, As Pontes Fault; NA, Narcea Antiform. Major variscan and alpine structures are depicted and the predominant rock type zonation represented in color.

flat until the continental slope, where sharply decreases to 18 km in 40 km distance to become oceanic crust beneath the abyssal plain (Fernández-Viejo et al., 1998). The study area belongs in terms of rift domain characterization to the proximal domain, where minor lithospheric thinning was achieved and small half-graben basins are formed (Cadenas et al., 2018).

The thickness of the seismogenic zone in the continental sector is estimated in 20 km (López-Fernández and Llana-Fúnez, 2015). The seismicity pattern is divided into a western sector where earthquakes tend to cluster in swarms and an eastern sector where seismicity is distributed. This seismic domains division matches the division in the tectonic style of structures accommodating the Alpine convergence: two systems of subvertical strike-slip faults to the West, contrasting to orogenic frontal thrusts to the East. The transit between both structural domains is aligned North-South and coincides with a local increase in seismic activity (**Figure 2**).

The Ventaniella-Cantabrian Fault System

The VF and CF system has a surface trace in geological maps that can be followed for more than 300 km crossing the CM and NIM in a NW–SE conspicuous trend, affecting Paleozoic and Mesozoic materials (**Figure 1**). Tavani et al. (2011) considered the VF as part of a 15 km wide shear zone including also the Ubierna fault in its southeastern termination, increasing further its length. Although the cartographic pattern is straightforward through the Paleozoic formations onshore, which are steeply dipping, its recognition becomes more challenging through the Mesozoic units, which are flat lying and not so well exposed. There are parts of the fault onshore that reactivate Permian extensional structures, as the main fault bounds some of the small Permian basins (Martínez-García et al., 2004), and others that reactivate earlier Variscan structures (Alonso et al., 2009). The movements and evolution along the long-stretched history are not fully understood. Nevertheless, its latest amply recognized movement corresponds to an oblique dextral fault with a reverse component, which resulting in a slight elevation of the NE block (Julivert et al., 1971; Julivert, 1976). There is also geomorphic evidence of quaternary movements, as it offsets Early Pleistocene alluvial fan deposits (Nozal and Gracia, 1990). According to these authors, the fault is sealed by younger fans, middle to upper Pleistocene in age. Its recent accumulated movement is also recorded in the coastal area, where the fault elevated 50 m a sector of the emerged wave cut platform that follows closely the North Iberian coast (López-Fernández et al., 2020). Across the mountain belt, it is also described to control the

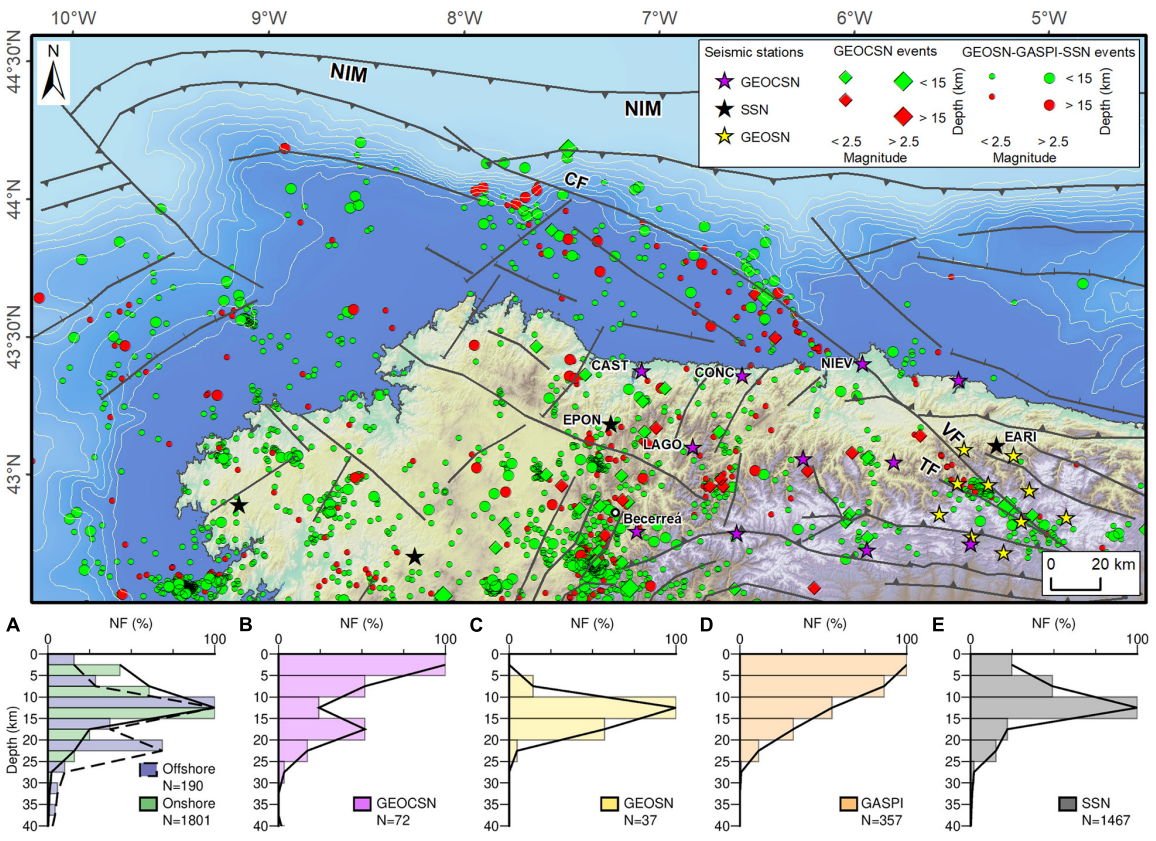

FIGURE 2 | DEM of the Cantabrian Mountains and North Iberian Margin with the seismicity and seismic networks available for the study. SSN, Spanish Seismic Network; GEOSN, Geocantabrica Seismic Network; GEOSCSN, GeocanCosta Seismic Network. The events are differentiated according to their depth and magnitudes with colors and sizing separating microevents from the rest (>2.5). Below, histograms representing the frequency distribution of the registered earthquakes with depth, **(A)** offshore and onshore depth distribution of events, **(B)** GEOSCN events, **(C)** GEOSN events, **(D)** GASPI events, and **(E)** SSN events.

asymmetric distribution of rivers and a secondary water shed (Jiménez-Sánchez, 1999).

Field data from the VF trace indicate a subvertical dip (Nozal and Gracia, 1990; Tavani et al., 2011). The seismicity onshore associated with its trace points to a minimum depth of 20 km for parts of the fault (**Figure 2**; López-Fernández et al., 2018). Offshore, it has been suggested that it could affect the whole crust (Cadenas et al., 2018). Regarding its activity, on the basis of seismic hazard calculations, the slip rate varies between 0.1 and 0.01 mm/year. Its dimensions make plausible the nucleation of an earthquake up to 7 magnitude, but considering the recurrence interval of more than 30 kyr, it is not regarded as a hazardous structure (Villamor et al., 2012).

Traditionally, the fault prolongation within the continental platform of the NIM followed the direction of the Aviles canyon, one of the deepest submarine valleys in the Atlantic (Gómez-Ballesteros et al., 2014). However, the study of Fernández-Viejo et al. (2014), remapped it with a strike of N60W and accompanied by a secondary branch striking N65W for at least another 80 km length. A large submarine slide was observed associated to its trace on the slope rim. This mass of material produced a bend in the trajectory of the Aviles canyon, which shows a weaker tectonic control than previously assumed.

The role of the CF–VF as a crustal domain boundary structure applies to seismicity, practically absent to the East (**Figures 2,4**), and to lithospheric and crustal thickness variations based on seismic refraction data, potential field modeling, and tomographic studies (Villaseñor et al., 2007; Torne et al., 2015; Palomeras et al., 2017; López-Fernández et al., 2018; Acevedo et al., 2020).

One striking aspect of the VF as a large-scale crustal feature is its modest accumulative apparent offsets. The strike slip 5 km offset (Julivert, 1976) or the 50 m vertical offset (López-Fernández et al., 2020), are well below 2% of its reported length and can be regarded as disproportionally low for a crustal-scale boundary. A question still to be answered is whether the fault moved in opposite senses throughout its long-lived history for longer distances, and only allows seeing the destructive interference of these movements. In summary, the transit between the drastic change in crustal properties on either side of the fault system remains enigmatic given the relatively small offset observed at the surface.

METHODS

In this contribution, we focus on the distribution of the offshore seismicity at the western NIM, and particularly that associated to the CF trace at sea, based on data from different available seismic networks. Data from the permanent Spanish seismic network, (SSN) and three portable local seismic networks have been analyzed in order to complete the offshore study. Two of these were deployed specifically to target the Ventaniella fault seismic segments (**Figure 2**):

(1) In September 2015, we deployed a dense short-period seismic array consisting of 10 stations around the active southern sector of the Ventaniella fault (Geocantabrica seismic network, GEOSN). The seismic stations were equipped with Worldsensing-Spidernano data loggers in combination with three-component 2 Hz Geospace MiniSeisMonitor sensors. This deployment registered for 19 months, covering an area of 60 km × 50 km (López-Fernández et al., 2018; Acevedo et al., 2020).

(2) Later, in May 2019, we installed a second seismic network covering a wider area in the Cantabrian Mountains (160 km × 80 km). This array (Geocantabrica-Costa seismic network, GEOCSN) was composed of 11 broadband seismic stations, 4 of which were placed along the coast in order to improve earthquake detection in the shelf. The seismic data was acquired using Nanometrics Taurus dataloggers along with Nanometrics Trillum 120 s sensors for a period of ∼9 months. Our datasets were complemented with waveforms from the two broadband stations of the SSN located in the area: EPON and EARI (**Figure 2**). Both the GEOSN and the GEOCSN arrays recorded continuous data at a sample rate of 100 Hz and were time-synchronized via Global Positioning System. The power supply was provided by solar panels when the connection to a wired electricity supply was not available. Some of the stations were accessed via a gateway modem for telemetry and data transmission.

The aim was to better localize and understand the continuous seismicity. Given the higher density in these local networks, it allowed us to increment the threshold of recording the events, and therefore improve their location. For example, the SSN registered 50 events in the same period than the local networks registered 72. Apart from the recent local GEOCSN and GEOSN networks, data from an earlier local deployment GASPI (**Figure 2**) have also been included in the study

Data processing was done with SEISAN software (**Figure 3**; Havskov et al., 2020). The detection of events within the continuous recordings was performed through a STA/LTA algorithm (STA length = 0.3 s; LTA length = 60 s; min. trig. duration = 1.5 s; min. trig. interval = 15 s; filter = 2–16 Hz), selecting events that had been registered by at least three of the stations. After identifying the local events of natural origin, the seismic phases were picked manually. Two examples from two earthquakes are shown in **Figure 3**. To locate the hypocenters, we used the HYPOCENTER program (Lienert et al., 1986; Lienert, 1991; Lienert and Havskov, 1995) and obtained in each case their ML and Mw magnitudes. The velocity model used was a 1D model of seven layers with a VP/VS ratio of 1.74, based on earlier studies and crustal structure local models (López-Fernández et al., 2018). The events magnitude MD was calculated with the formula of Lee and Lahr (1975) for local earthquakes.

The average error in localization from the local networks in X (north), Y (East), and Z (depth) directions are respectively 4.6, 3.7, and 8.3 km, while values of 6.81, 3.76, and 6.51 are given by the SSN in the period 1980–2021 (**Figure 4**).

The registered local earthquakes were integrated into a database implemented in a Geographic Information System, which allows the visualization, analysis, and spatial management of all the seismic information generated.

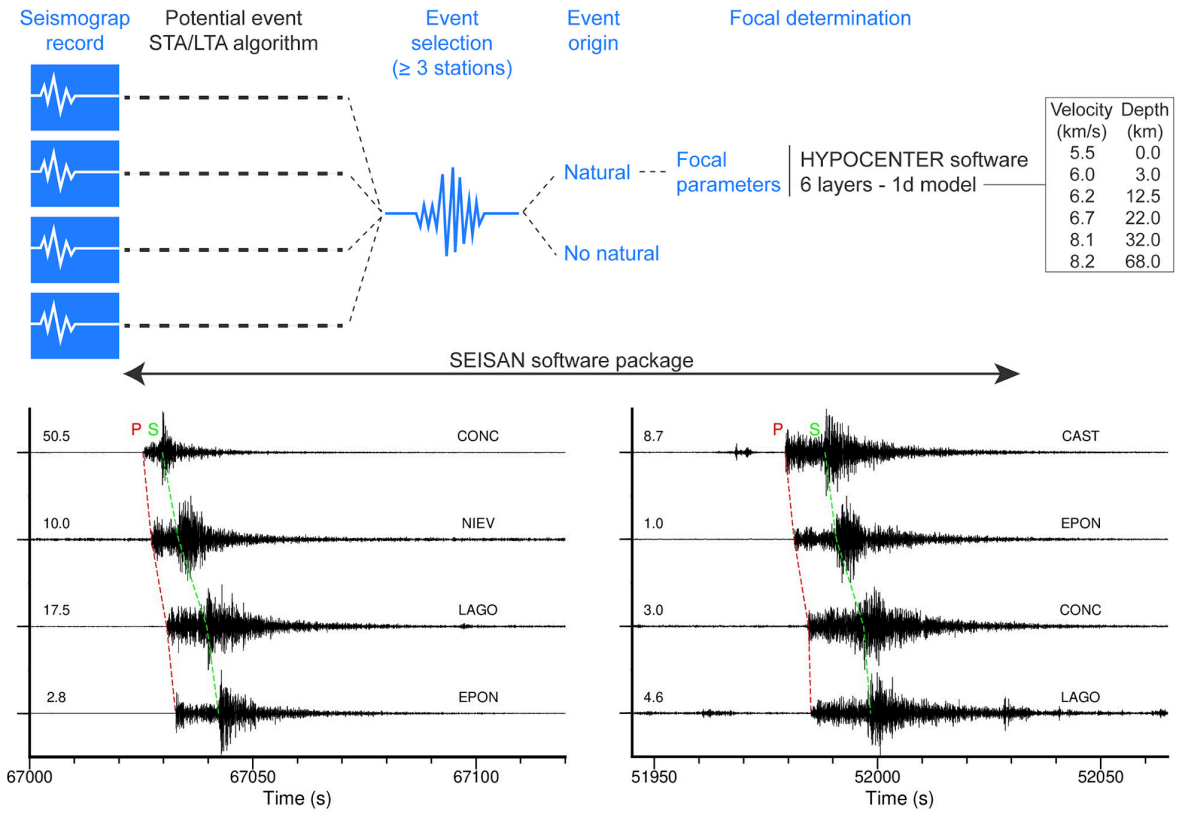

FIGURE 3 | Processing scheme followed to locate the seismic events. Below, examples of waveforms recorded for a **(left)** M_L 2.7 earthquake that occurred on December 8, 2019 (18:36 UTC) and a **(right)** M_L 2.5 earthquake registered on June 22, 2019 (14:26 UTC). Numbers of the left refer to the amplitude of the traces in counts × 10^3. Time is expressed in hour of the day in seconds. P and S-wave arrivals marked in red and green respectively.

RESULTS: DISTRIBUTION OF EARTHQUAKES IN THE CONTINENTAL PLATFORM

The coastal network was deployed with the double objective of improving the accuracy of the continental platform events, and with the aim of obtaining tomographic models through interferometry of ambient noise (Acevedo et al., 2019). The number of earthquakes registered at the shelf from all networks amounts to 195 events between longitudes 5 and 9° 30′ W in a period of two decades. During four of those years, the three temporary networks were deployed (GASPI, GEOSN, and GEOCSN). However, considering the scarce instrumental cover in the region it is reasonable to think that the number of events is largely underestimated.

The improvement in detection of events and specially the proximity of the receiving stations from GEOSCN to the offshore areas increased the available data to depict a first map of the distribution of earthquakes in the marine segment of the fault up to date. Overall, 37 local events between September 2015 and March 2017 were extracted from the GEOSN dataset (López-Fernández et al., 2018). Due to the enhancement of the detection capability generated by the short inter-station distances of the GEOSN network, 35 of these events were not previously registered in the SSN catalogs. Later, the GEOCSN network contributed to the addition of another 73 local earthquakes, 24 of which were previously undetected. Specifically GEOCSN detected 7 offshore earthquakes between 6 and 21 km depth with magnitudes between 1.9 and 2.9.

The seismic catalog was complemented with events from the GASPI network, which operated between 1999 and 2002 (López-Fernández et al., 2012), which delivered 14 earthquakes close to Aviles, between 9 and 20 km and average magnitude 2,2. It also delivered 8 more earthquakes with a disperse distribution and average magnitude of 2.5. With respect to the SSN, we have extracted 64 events with a disperse distribution and average magnitude of 2.1 in the further offshore areas and 91 events closer to the coast with an average magnitude of 2.4.

Comparing with the inland earthquakes, the number of events offshore is lower but for some of the events, their depth seems considerably higher.

The spatial distribution of earthquakes, both offshore and onshore, is shown in map view in **Figure 2** and along swath vertical profiles in **Figure 4**. Offshore, the epicenters show a NW–SE trend approximately coincident with the trace of the CF, all within the southern crustal block (**Figures 1**, **2**).

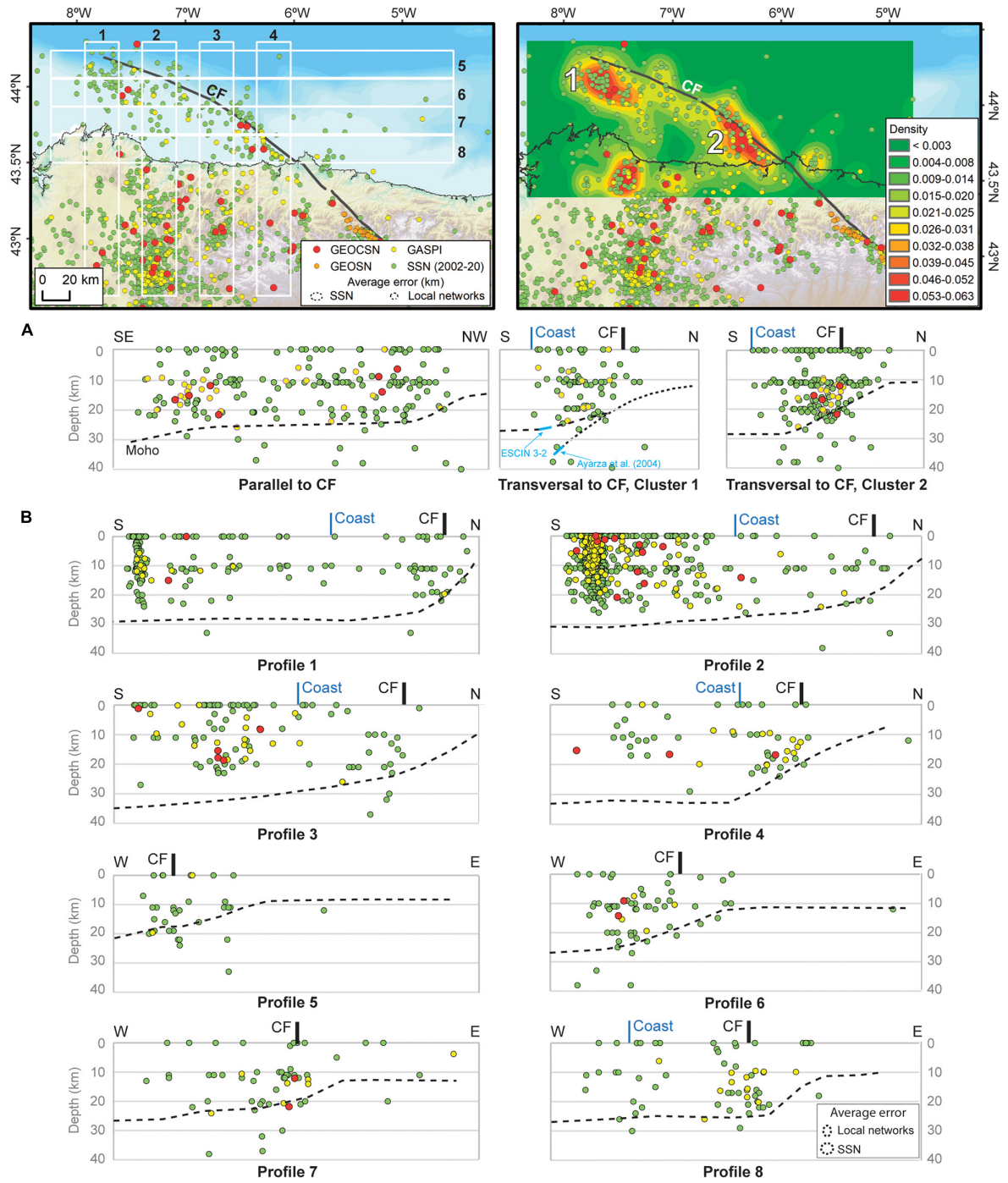

FIGURE 4 | (Left) distribution of the seismicity along the study area with location of swath profiles 1–8 and average error ellipses and **(right)** heat map showing the clusters of seismicity obtained through a density estimation statistical analysis (fourth degree kernel function, area chosen 450 m). **(A)** Seismicity profiles along VF-CF strike and perpendicular to it along Clusters 1 and 2. In light blue are represented in the cluster 1 the Moho and sub-Moho reflections according to Ayarza et al. (2004) which could indicate the presence of the top of the Biscay slab **(B)** Swath depth profiles 1–4, in S–N direction, 5–8 in W–E. The depth to the crust-mantle boundary has been plotted in the profiles (from Cadenas et al., 2018) to contextualize the seismicity. The average error ellipses are indicated in the right corner of the last profile for both, local and SSN networks.

The inset in **Figure 2** shows the frequency distribution of events with depth, which is a graphical proxy to deduce the seismogenic thickness of the study area (e.g., Tavani et al., 2020). Even considering the higher error in hypocentral location, therefore trying to be cautious, the seismicity onshore and offshore presents a clear distinction: while the onshore events

are distributed along the seismogenic crust, with a maximum between 10 and 15 km depth, for the offshore events there is two maxima in the distribution pointing out to two different origins of the earthquakes. The first maxima is again located at mid crustal depths of 12, but the second one is much deeper being located at around 20–25 km depth.

A heat map of earthquakes foci along the continental platform of the western NIM portrays the presence of two preferential areas for earthquakes occurrence, one for about 40 km at the end of the continental platform in the NW (Cluster 1 in **Figure 4**) and a second one, close to the coast (Cluster 2 in **Figure 4**). The density distribution also shows a small cluster onshore at around longitude 7.5° W, coinciding with the presence of a normal fault trending northeasterly, that could potentially be the triggering structure for the observed seismicity.

Figure 4B displays the distribution of the same events with depth projected in four S–N and four W–E swath profiles whose location is given in **Figure 4**. All profiles portray the projection of the estimated Moho depth (Cordoba et al., 1988; Ayarza et al., 1998; Fernández-Viejo et al., 1998; and compiled in Cadenas et al., 2020) for a crustal depth contextualization. South to North profiles, 1–4 in **Figure 4B**, also include the onshore seismicity for reference. The denser continental clusters correspond to the ones along the As Pontes fault and the so-called Becerreá swarm inland (**Figures 1,2**; López-Fernández et al., 2012).

The effect of the CF-VF system offshore is particularly noticeable in the W-E swath profiles, numbered 5–8 in **Figure 4B**, where one can observe that events practically disappear on the northeastern crustal block. These latitudinal swath profiles illustrate clearly the boundary effect exerted by the CF–VF, separating two very contrasting crustal blocks according to the seismic record. The southernmost swath shows the influence of the continental seismicity in the southern crustal block, which is more evenly distributed and related to other local structures. The distribution follows the NW–SE trend of the fault system but clustering in two sectors. The figure also shows the distribution of seismicity in cross-section along the trace of the fault in NW–SE direction, containing most of the offshore events, and two perpendicular sections to the main fault along the two clusters.

DISCUSSION: SEISMICITY PATTERN OF THE WESTERN NIM

The drastic change in crustal thickness in the NIM from the continent toward the abyssal plain is similar to the one found in active margins, a morphological reminiscence of the short-lived subduction that took place during the Alpine convergence (e.g., Álvarez-Marrón et al., 1997). This confers to the NIM its somewhat atypical abruptness for a passive margin profile. From the vertical profiles in **Figure 4B**, it is clearly seen the constant thickness of the seismogenic zone onshore, while increasing slightly toward the N, even as the crust is getting thinner toward the abyssal plain.

The alignment of cluster 1 with the CF may be caused in the same way as in the 70 km long seismic segment of the VF inland (López-Fernández et al., 2018), that is, as an intersection between two structures, the CF, and a south-dipping, East-West trending one. The existence of an inherited weak interface at the foot of the continental margin, in favorable orientation to interact with other structures in the crust above, is therefore a strong candidate to help nucleate part of the seismicity recorded around the CF. A potential candidate for such structure is the arrested subduction plane of the Bay of Biscay (Álvarez-Marrón et al., 1997; Ayarza et al., 2004). The regional context provides this alternative scenario as it is assumed that a plane of underthrusting was created when the Bay of Biscay oceanic crust, due to the collision of Iberia and Europe, started to be consumed beneath the NIM. The depth of this interface is poorly constrained, but Ayarza et al. (2004), interpreted a series of sub-Moho arrivals in a deep seismic reflection profile as out of the plane reflections from the top of the presumed subducted slab situated at 40 km depth near the coastline and dipping 45° (**Figure 4A**, transversal to CF, cluster1). At the latitude of cluster 1, if we extrapolate from that depth and dip, the top of this plane should be encountered at around 25 km depth, which agrees with the depth of some of the cluster 1 earthquakes. In fact, these events correspond to the second maxima in the frequency distribution inset (**Figure 2**). Thus, there is scope in the future to constrain better this particular area of structural intersection, pending on an improvement in earthquake location to support this hypothesis.

Profile 8 in **Figure 4B** portrays a second elongated cluster near the coast, strongly following the CF on its southern crustal block. The seismogenic zone involves the full thickness of the crust, suggesting that the whole crust would be locally behaving in a brittle manner. Nevertheless, close to the cluster 2 onland, the area around the Narcea Antiform (NA) localizes deep seismicity (**Figure 1**). The NA constitutes the boundary between the external and internal zones of the Variscan orogen and it is characterized by involving the crystalline basement during the Variscan thrusting (Pérez-Estaún et al., 1991). The presence at or near the surface of gneisses and various pre-Variscan igneous rocks (Rubio-Ordóñez et al., 2015) points to its role as a rigid body with respect to surrounding relatively softer materials: a slate belt to the West, and a sedimentary rock sequence to the East in the Variscan foreland-fold-and-thrust belt. The lateral continuation of the NA toward the NE intersecting the CF coincides broadly with the more populated cluster 2 in the NIM.

We have so far seen that the two offshore clusters identified in this contribution have three things in common: (a) they are aligned with the CF, a crustal-scale structure given the range of depths at which activity occurr, (b) they appear where other crustal scale structures intersect the trace of the CF, and (c) they mostly nucleate in the southern block. The structure of the crust in this block is characterized by the strong imprint imposed during the Variscan orogeny and the minimum tectonothermic imprint during the alpine cycle (Cadenas et al., 2018). On the one hand, the grain of the orogen, which may be regarded as a crustal fabric, is orthogonal to the CF. On the other hand, the nature of the rocks in the vicinity of the clusters is dominated by either high grade metamorphic rocks (cluster 1) or by old crystalline igneous rocks (cluster 2). The conjunction of the two factors, crustal fabric and rock type, suggests a stronger basement. This

lateral gradient in crustal strength, would favor the concentration and amplification of stresses in the western sector, stresses that would be released on a bounding pre-existing and relatively weak structure, such as the CF–VF system may be regarded.

In summary, the intersection of the NW-SE trending major structure whether with W–E trending compressional structures or with inherited variscan discontinuities, together with the stronger basement provides a favorable setting where the concentration of stress may accumulate sufficient energy in an intraplate scenario to be released rapidly producing the observed seismicity patterns.

CONCLUSION

Based on the seismological study of events recorded on local seismic networks focused on the VF–CF system complemented with earlier available data, a map of earthquake activity along the western continental platform of the NIM is presented. The location and distribution of earthquakes confirm their origin as linked to the presence of the fault at sea. However, there are several contributing factors as to why this structure nucleates the observed seismicity only around some segments of its trace. As suggested onshore, the intersection of the CF with other crustal scale structures, is one possible scenario for the offshore earthquakes. In the vicinity of the abyssal plain at the NW end, the seismicity cluster could be related to the arrested subduction during the Alpine convergence, while closer to the coast, it could be the interaction with reactivated Variscan structures oriented favorably for the current state of stress.

The offshore study reinforces the onshore observation that the CF–VF system is an important barrier separating two crustal blocks according to their seismicity: a western block, with moderate, low-magnitude but persistent seismicity, and an eastern block where is practically absent. This is possibly the result of the different types of crust at one side and another, with different tectonothermal regimes through the Mesozoic and contrasting degrees of deformation during the Cenozoic convergence. The presence of crystalline Variscan basement barely affected by the Mesozoic extensions and posterior convergence makes an outstanding candidate to produce a sharp contrast in the mechanical behavior of the crusts on either side of the fault. The brittle behavior of the Western crustal block may be envisaged as reflecting its stronger mechanical strength, in contrast with the weaker ductile Eastern crustal block.

The VF–CF system behaves as a full crustal scale discontinuity that when encountering other crustal heterogeneities concentrates and amplifies the mechanical contrast, due to its favorable position within the actual stress state of the Northwest Iberian Peninsula. Our analysis reinforces the need for seismological studies constraining better the north azimuths to test the various hypothesis proposed here. Any future improvement in the resolution of events location will eventually translate into major constrains of the details of structures nucleating seismicity

DATA AVAILABILITY STATEMENT

The GEOSN dataset (2M, doi: 10.7914/SN/2M_2015) analyzed for this study is available online at the Observatories and Research Facilities for European Seismology (ORFEUS) Data Center (http://www.orfeus-eu.org/). The GEOCSN dataset (YR, doi: 10.7914/SN/YR_2019) analyzed for this study can be released to the public on demand at GEOCANTABRICA@ftp.geol.uniovi.es. Additional data from stations EARI and EPON are courtesy of the Instituto Geográfico Nacional (www.ign.es).

AUTHOR CONTRIBUTIONS

All authors listed have made a substantial, direct and intellectual contribution to the work, and approved it for publication.

FUNDING

This work was financed through projects: GRUPIN14-044, GRUPIN18-00184, and CGL2017-86487-P. JA holds a *Severo Ochoa* predoctoral Grant from the Government of Asturias (PA-17-PF-BP-16139).

ACKNOWLEDGMENTS

We thank the local people and institutions that helped to install the seismic networks in Asturias, Galicia and León. Mario Ruiz and Jordi Díaz from the Labsys in Geo3bcn for providing instruments and support during the recordings. We also thank the IGN for sharing the datasets of stations EARI and EPON.

REFERENCES

Acevedo, J., Fernández-Viejo, G., Llana-Fúnez, S., López-Fernández, C., and Olona, J. (2019). Ambient noise tomography of the southern sector of the Cantabrian mountains, NW. Spain. *Geophys. J. Int.* 219, 479–495. doi: 10.1093/gji/ggz308

Acevedo, J., Fernández-Viejo, G., Llana-Fúnez, S., López-Fernández, C., and Olona, J. (2020). Upper crustal seismic anisotropy in the Cantabrian mountains (North Spain) from shear-wave splitting and ambient noise interferometry analysis. *Seism. Res. Lett.* 9, 421–436. doi: 10.1785/0220200103

Alonso, J. L., Marcos, A., and Suárez, A. (2009). Paleogeographic inversion resulting from large out of sequence breaching thrusts; the Leon fault (Cantabrian Zone, NW Iberia). a new picture of the external variscan thrust belt in the Ibero Armorican. *Arc. Geol. Acta* 7, 451–473.

Álvarez-Marrón, J., Rubio, E., and Torne, M. (1997). Subduction related structures in the north iberian Margin. *J. Geophys. Res.* 102, 22497–22511. doi: 10.1029/97jb01425

Arche, A., and López-Gómez, J. (1996). Origin of the permian-triassic iberian basin, central-eastern Spain. *Tectonophysics* 266, 443–464. doi: 10.1016/s0040-1951(96)00202-8

Ayarza, P., Catalán, J. R. M., Álvarez-Marrón, J., Zeyen, H., and Juhlin, C. (2004). Geophysical constraints on the deep structure of a limited ocean-continent subduction zone at the North Iberian Margin. *Tectonics* 23:TC1010.

Ayarza, P., Catalán, J. R. M., Gallart, J., Pulgar, J. A., and Dañobeitia, J. J. (1998). Estudio sísmico de la Corteza Ibérica Norte 3.3. a seismic image of the variscan crust in the hinterland of the NW Iberian Massiff. *Tectonics* 17, 171–181. doi: 10.1029/97tc03411

Boillot, G., Dupeuble, P. A., and Malod, J. (1979). Subduction and tectonics on the continental margin off northern Spain. *Mar. Geol.* 32, 53–70. doi: 10.1016/0025-3227(79)90146-4

Cadenas, P., Fernández-Viejo, G., Pulgar, J. A., Tugend, J., and Manatschal, G. (2018). Constraints imposed by rift inheritance on the compressional reactivation of a hyperextended margin: mapping rift domains in the North Iberian margin and in the Cantabrian Mountains. *Tectonics* 37, 758–785. doi: 10.1002/2016tc004454

Cadenas, P., Manatschal, G., and Fernández-Viejo, G. (2020). Unravelling the architecture and evolution of the inverted multi-stage North Iberian–bay of biscay rift. *Gond. Res.* 88, 67–87. doi: 10.1016/j.gr.2020.06.026

Cordoba, D., Banda, E., and Ansorge, J. (1988). P-wave velocity depth distribution in the Hercynian crust of northwest Spain. *Phys. Earth Planer. Int.* 51, 235–248. doi: 10.1016/0031-9201(88)90050-7

Fernández Viejo, G., Gallart, J., Pulgar, J. A., Córdoba, D., and Dañobeitia, J. J. (2000). Seismic signature of Variscan and alpine tectonics in NW Iberia: crustal structure of the Cantabrian Mountains and Duero Basin. *J. Geophys. Res.* 105, 3001–3018. doi: 10.1029/1999jb900321

Fernández-Viejo, G., Gallart, J., Pulgar, J. A., Gallastegui, J., Dañobeitia, J. J., and Cordoba, D. (1998). Crustal transition between continental and oceanic domains along the North Iberian Margin from wide angle seismic and gravity data. *Geophys. Res. Lett.* 25, 4249–4252. doi: 10.1029/1998gl900149

Fernández-Viejo, G., López-Fernández, C., Domínguez-Cuesta, M. J., and Cadenas, P. (2014). How much confidence can be conferred on tectonic maps of continental shelves? the Cantabrian fault case. *Sci. Rep.* 4:3661.

Fernández-Viejo, G., Pulgar, J. A., Gallastegui, J., and Quintana, L. (2012). The fossil accretionary wedge of the Bay of Biscay: critical wedge analysis on depth migrated seismic sections and geodynamical implications. *J. Geol.* 120, 315–331. doi: 10.1086/664789

Gómez-Ballesteros, M., Druet, M., Muñoz, A., Arrese, B., Rivera, J., Sánchez, F., et al. (2014). Geomorphology of the Aviles canyon system, Cantabrian Sea (Bay of Biscay). *Deepsea Res. Part II* 106, 99–117. doi: 10.1016/j.dsr2.2013.09.031

Havskov, J., Voss, P. H., and Ottemoller, L. (2020). Seismological observatory software: 30 yr of SEISAN. *Seism. Res. Lett.* 91, 1846–1852. doi: 10.1785/0220190313

Jiménez-Sánchez, M. (1999). Geomorfología fluvial en la cabecera del río Nalón (Cordillera Cantábrica, Noroeste de España). *Trab. Geol.* 21, 189–200.

Julivert, M. (1976). La ventana del río Monasterio y la terminación meridional del manto del Ponga. *Trab. Geol.* 1, 59–76.

Julivert, M., Ramírez, del Pozo, J., and Truyols, J. (1971). *Histoire Structurale du Golfe de Gascogne*. Paris: Technip.

Lee, W. H. K., and Lahr, J. C. (1975). HYPO71 (revised): a computer program for determining hypocenter, magnitude and first motion pattern of local earthquakes, U.S. *Geol. Surv. OFR* 75–311, 1–116.

Lienert, B. R. E. (1991). *Report on Modifications Made to Hypocenter, Institute of Solid Earth Geophysics*. Norway: University Bergen.

Lienert, B. R. E., and Havskov, J. (1995). A computer program for locating earthquakes both locally and globally. *Seism. Res. Lett.* 66, 26–36. doi: 10.1785/gssrl.66.5.26

Lienert, B. R. E., Berg, E., and Fraser, L. N. (1986). HYPOCENTER: and earthquake location method using centered, scales, and adaptively damped least squares. *Bull. Seism. Soc. Am.* 76, 771–783.

López-Fernández, C., and Llana-Fúnez, S. (2015). The seismogenic zone of the continental crust in Northwest Iberia and its relation to crustal structure. *Tectonics* 34, 1751–1767. doi: 10.1002/2015tc003877

López-Fernández, C., Fernández-Viejo, G., Olona, J., and Llana-Fúnez, S. (2018). Intraplate seismicity in Northwest Iberia along the trace of the ventaniella fault: a case for fault intersection at depth. *Bull. Seism. Soc. Am.* 108, 604–618. doi: 10.1785/0120170215

López-Fernández, C., Llana-Fúnez, S., Fernández-Viejo, G., Domínguez-Cuesta, M., and Díaz-Díaz, L. M. (2020). Comprehensive characterization of elevated coastal platforms in the North Iberian Margin: a new template to quantify uplift rates and tectonic patterns. *Geomorphology* 364:107242. doi: 10.1016/j.geomorph.2020.107242

López-Fernández, C., Pulgar, J. A., Díaz, J., Gallart, J., González-Cortina, J. M., and Ruiz, M. (2012). Seismotectonic characterization of the Becerrea área (NWSpain). *Geol. Acta* 10, 71–80.

López-Sánchez, M., and Llana-Fúnez, S. (2018). A cavitation –seal mechanism for ultramylonite formation in quartzofeldspathic rocs within the semibrittle field (Vivero fault, NW Spain). *Tectonophysics* 745, 132–153. doi: 10.1016/j.tecto.2018.07.026

Martínez-García, E., Anotania, J. F., García-Sanchez, A., and Quiroga de la Vega, J. L. (2004). Tectonic and metallogenic significance of sedimentary manganese deposits in the eastern cantabrian domain Asturias, Northwestern Spain. *Int. Geol. Rev.* 46, 273–288. doi: 10.2747/0020-6814.46.3.273

Nozal, F., and Gracia, F. J. (1990). El Piedemonte de la Sierra del Brezo (Montes Palentinos). *Actas 1.ª Reunión Nacional de Geomorfología*. Teruel, 763–772.

Palomeras, I., Villaseñor, A., Thurner, S., Levander, A., Gallart, J., and Harnafi, M. (2017). Lithospheric structure of Iberia using finite-frequency Rayleigh wave tomography from earthquakes and seismic ambient noise. *Geochem. Geophys. Geosys.* 18, 1824–1840. doi: 10.1002/2016gc006657

Pérez-Estaún, A., Catalán, J. R. M., and Bastida, F. (1991). Crustal thickening and deformation sequence in the footwall to the suture of the variscan belt of northwest Spain. *Tectonophysics* 191, 243–253. doi: 10.1016/0040-1951(91)90060-6

Roca, E., Muñoz, J. A., Ferrer, O., and Ellouz, N. (2011). The role of the bay of biscay Mesozoic extensional structure in the configuration of the Pyrenean orogeny: constraints from the Marconi deep seismic reflection survey. *Tectonics* 30:TC2001.

Rubio-Ordóñez, A., Gutiérrez-Alonso, G., Valverde-Vaquero, P., Cuesta, A., Gallastegui, G., and Gerdes, A. (2015). Arc-related ediacaran magmatism along the northern margin of Gondwana: geochronology and isotopic geochemistry from northern Iberia. *Gond. Res.* 27, 216–227. doi: 10.1016/j.gr.2013.09.016

Srivastava, S. P., Schouten, H., Roest, W. R., Klitgord, K. D., Kovacs, L. C., Verhoef, J., et al. (1990). Iberian plate kinematics. a jumping plate boundary between Eurasia and Africa. *Nature* 344, 756–759. doi: 10.1038/344756a0

Stern, R. J., and Gerya, T. (2018). Subduction initiation in nature and models: a review. *Tectonophysics* 746, 173–198. doi: 10.1016/j.tecto.2017.10.014

Tavani, S., Camanni, G., Nappo, M., Snidero, M., Ascione, A., Valente, E., et al. (2020). The mountain front flexure in the Luresan región of the Zagros belt: crustal architecture and role of structural inheritances. *J. Struct. Geol.* 135:104022. doi: 10.1016/j.jsg.2020.104022

Tavani, S., Quinta, A., and Granado, P. (2011). Cenozoic right-lateral wrench tectonics in the Western Pyrenees (Spain). the Ubierna fault system. *Tectonophysics* 509, 238–253. doi: 10.1016/j.tecto.2011.06.013

Torne, M., Fernández, M., Verges, J., Ayala, C., Salas, M. C., Jimenez-Munt, I., et al. (2015). Crust and mantle lithospheric structure of the Iberian Peninsula deduced from potential field modelling and thermal analysis. *Tectonophysics* 663, 419–433. doi: 10.1016/j.tecto.2015.06.003

Tugend, J., Manatschal, G., Kusznir, N. J., Masinsi, E., Mohn, G., and Thinon, I. (2014). Formation and deformation of hyperextended rift systems: insights from rift domain mapping in the Bay of Biscay-Pyrenees. *Tectonics* 33, 1239–1276. doi: 10.1002/2014tc003529

Villamor, P., Capote, R., Stirling, M. W., Tsige, M., Berryman, K. R., Martínez-Díaz, J. J., et al. (2012). Contribution of active faults in the intraplate area of Iberia to seismic hazard: the Alentejo-Plasencia fault. *J. Iberian Geol.* 38, 85–111.

Villaseñor, A., Yang, Y., Riztwoller, M. H., and Gallart, J. (2007). Ambient noise surface wave tomography of the Iberian Peninsula: implications for shallow seismic structure. *Geophys. Res. Lett.* 34:L11304.

Conflict of Interest: The authors declare that the research was conducted in the absence of any commercial or financial relationships that could be construed as a potential conflict of interest.